

Quantized electron transport through a time-dependent potential barrier

P. A. Maksym

Department of Physics and Astronomy, University of Leicester, University Road, Leicester LE1 7RH, United Kingdom

(Received 30 April 1999; revised manuscript received 8 September 1999)

Electron transport by a potential minimum that moves through a barrier is investigated numerically and theoretically. The integrated electron transfer as a function of the Fermi level has a series of plateaus, each of which corresponds to an integral number of electrons. The accuracy of the quantization depends on the barrier height and can be 1 part in 10^{10} or better. The transport mechanism involves nonadiabatic Landau-Zener transitions.

Time-dependent quantum systems, which could serve as a new standard of electrical current, are coming under increasing scrutiny. If there was a system which could transfer an integral number of electrons per cycle when its Hamiltonian was changed periodically, it would function as a frequency to current converter, giving an accurate standard of current when driven with an accurately known frequency. Although the combination of speed and accuracy required for metrology (above 1 GHz and between 1 part in 10^7 and 10^8) has not yet been reached, there are two promising approaches. One is to construct the system from a chain of small metallic islands coupled by quantum tunnel junctions.¹ Another is to transport electrons in the potential minima of a surface acoustic wave (SAW) propagating through a one-dimensional (1D) channel in a piezoelectric semiconductor.² A model inspired by this approach is investigated in the present work. The mechanism of electron transfer is found to involve nonadiabatic Landau-Zener transitions and the accuracy of the electron transfer is shown to be 1 part in 10^{10} or better.

The SAW device consists of a 1D GaAs channel that separates a 2D electron gas into two regions. SAWs propagate in the direction parallel to the channel and their potential is believed to be screened in the regions of high electron density on either side of the channel.³ Thus the SAW potential is only significant in the vicinity of the channel and the SAW generates a potential minimum that develops in strength and moves through the channel. Although transport through the device is probably influenced by the transition from 2D motion to 1D motion at the mouth of the channel and by electron-electron interactions, the time-dependent potential is essentially one dimensional. It seems that a prerequisite for accurate electron transfer in the device as a whole is accurate transfer of noninteracting electrons through a time-dependent channel at zero temperature and the purpose of this work is to investigate whether this is possible. The influence of other effects, such as interactions and finite temperature, is briefly discussed after the possibility of accurate electron transfer in the 1D noninteracting system has been established.

A 1D model potential consistent with the conditions in a SAW device is $V(x,t) = \exp(-x^2/a^2)[V_0 + U_0 \cos(kx - \omega t)]$, where V_0 is the height of the potential barrier between the two regions of high electron density, U_0 is the amplitude of the SAW potential, $k = 2\pi/\lambda$, $\omega = 2\pi/\tau$, and λ and τ are the SAW wavelength and period. Experimentally, the barrier

contains only one minimum of the SAW potential at $t \sim \tau/2$ and this condition is simulated by choosing $2a = \lambda$. The wavelength and frequency are chosen to be 1 μm and 1 GHz, similar to experimental values. The GaAs effective mass is used, $m^* = 0.067m_0$. For simplicity, most calculations are done with $U_0 = V_0$ and the effect of relaxing this assumption is discussed later.

The electron transfer per cycle is calculated by solving the time-dependent Schrödinger equation. The barrier is taken to be in the center of an enclosing box of width $L = 10 \mu\text{m}$ and the wave function is taken to vanish at the end points of the box. Initial states are found by diagonalizing the Hamiltonian with potential $V(x, t_0)$. The initial time t_0 is set to -0.001τ as a precaution against numerical problems with accurate calculation of $t = 0$ eigenstates which are highly degenerate, but the physics is insensitive to the precise value of t_0 . Each state is propagated for one period and the net electron transfer N is found by summing electron transfers for individual states up to the Fermi level:

$$N = \sum_{E_i(t_0) \leq E_F} \int_{L/2}^L |\psi_i(x, t_0 + \tau)|^2 - |\psi_i(x, t_0)|^2 dx. \quad (1)$$

Each state up to E_F is taken to be singly occupied. Double occupancy cannot be treated accurately without considering interaction of electrons in the SAW minimum.

Results for the electron transfer as a function of E_F are shown in Fig. 1. Each curve has a plateau or plateaus where the electron transfer is very close to an integer. For the low-

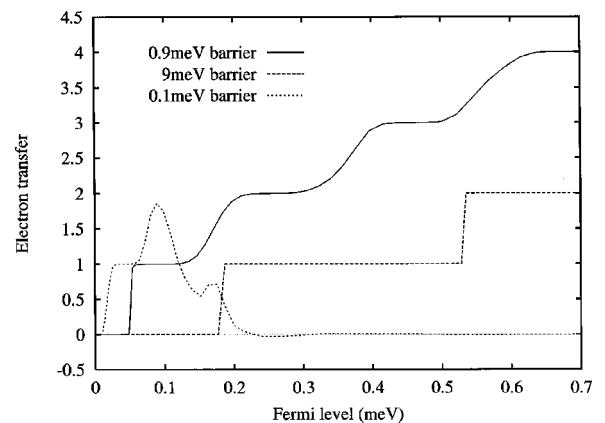


FIG. 1. Net electron transfer as a function of the Fermi level for various barrier heights.

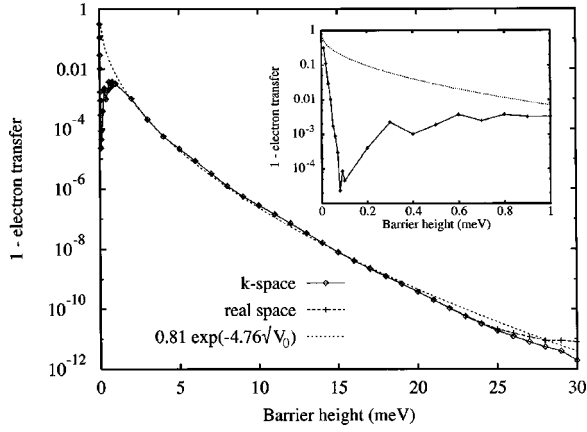


FIG. 2. Accuracy of quantization at plateau centers. The inset shows the low barrier regime.

est barrier height only one plateau is evident, then the electron transfer drops to zero as E_F increases. This is a consequence of unitarity. As E_F becomes large each of the two sums in Eq. (1) approaches the trace of $\theta(x - L/2)$. The trace is time invariant because the time evolution operator is unitary, therefore the two terms tend to cancel when there are sufficiently many states below E_F . For the larger values of V_0 , the cancellation does not occur in the energy range shown. The electron transfer occurs at relatively low E_F because $U_0 = V_0$; the first plateau shifts to higher E_F when U_0 is decreased.

Numerical investigation of the quantization accuracy requires N to be calculated to 1 part in 10^{10} or better. The Hamiltonian is discretized in real space with a finite difference approximation to the second derivative or in k space with a Fourier sine expansion. The time-dependent Schrödinger equation then becomes a system of ordinary differential equations which are solved numerically with automatic control of the space-time grid size. However, step size control procedures generally give control over local errors while the global error needs to be controlled to compute the electron transfer. To check the global error the calculations are done with both real and k -space discretization. The real and k -space programs are independent except for the function that calculates the potential and use of both approaches gives some protection against programming errors as well as global errors. Some calculations were done on two different computers as a precaution against system errors.

The accuracy of the first plateau as a function of V_0 is shown in Fig. 2. The accuracy is measured by $1 - N$ at the plateau center, where dN/dE_F has a minimum. The diamonds and crosses indicate the real and k -space results, respectively. For $V_0 < 23$ meV, the results for $1 - N$ agree to 3% and the agreement is better than 0.5% for $V_0 < 15$ meV. The two curves diverge when $V_0 > 23$ meV and this is probably due to a small normalization error ($\sim 10^{-11}$) which occurs in the real space calculation when a very fine grid is used. It is clear from the figure that there are two regimes. In the high barrier regime, $V_0 > 1$ meV, the accuracy improves smoothly with barrier height and is system size independent. In the low barrier regime the accuracy oscillates (see inset) and the form of the oscillations is sensitive to the system

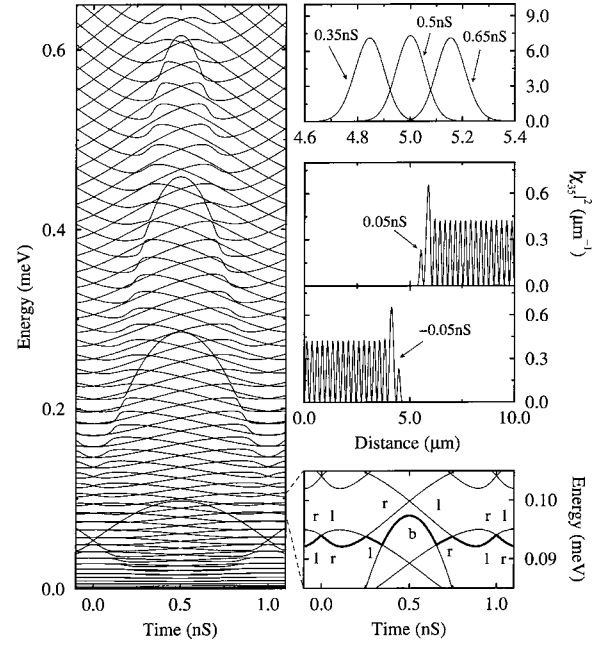


FIG. 3. Instantaneous eigenvalues and eigenstates for the 0.9 meV barrier. Left and bottom right frames: eigenvalues, bold line, eigenvalue 35; top right: eigenstate 35.

size. The accuracy in the high barrier regime is well fitted by $\alpha \exp(-\beta\sqrt{V_0})$ with $\alpha = 0.81 \pm 0.07$, $\beta = 4.76 \pm 0.05$.

To investigate the transport mechanism, the time-dependent wave functions are related to the instantaneous eigenstates χ_i of the Hamiltonian which obey $[p^2/2m^* + V(x, t)]\chi_i(x, t) = E_i(t)\chi_i(x, t)$. The eigenvalues $E_i(t)$ for $V_0 = 0.9$ meV are shown in the left hand frame of Fig. 3. Each level is nondegenerate, but there are many anticrossings at which the level splitting is too small to be resolved in the figure. Except for $t = 0$ and $t = \tau/2$, the instantaneous eigenstates are of propagating, left, right, or bound character. Propagating states occupy both sides of the barrier; left and right states occupy only one side of the barrier and bound states are localized in a potential minimum. For $t = 0$ and $t = \tau/2$, left and right states can be constructed from nearly degenerate symmetric and antisymmetric states. The character of each state is time dependent. The bound states correspond to the parabolic structures in the figure and the development of the lowest structure is shown on an expanded scale in the bottom right frame. State number 35 (bold energy level) is bound for $t \sim \tau/2$ and the characters of this state and state 36 are indicated at selected time points by the letters l , r , b . The top right frames show state 35 in its left, right, and bound phases and the topmost frame shows the localization of the bound state shifting from left to right at $t \sim \tau/2$. The character of all states changes at an anticrossing but only a few states are bound at $t \sim \tau/2$ and only these states are associated with a shift of localization from left to right. Anticrossing behavior that involves two levels is typical and also occurs for asymmetric barriers. More complicated behavior that involves more than two levels can occur by accident at special barrier heights.

The anticrossings influence the time evolution via Landau-Zener transitions⁴ between the two states entering and leaving the anticrossing. The probability of a Landau-Zener transition can be found by using a special basis in

which each state has the same character at all times⁴ but an approximate treatment in the instantaneous eigenstate basis, which does not seem to be in the literature, gives more insight into the numerical data. The two level Hamiltonian is found by Taylor expanding the potential about the anticrossing time, t_a . This gives the matrix elements $H_{11} = E_1(t_a)$, $H_{22} = E_2(t_a)$, and $H_{12} = m(t - t_a)$ where $m = \omega U_0 \langle \chi_1(t_a) | \exp(-x^2/a^2) \sin(kx - \omega t_a) | \chi_2(t_a) \rangle$. The evolving quantum state of the two level system is written in terms of *its* instantaneous eigenvalues and eigenstates, \tilde{E} and $\tilde{\chi}$, as $a_1(t) \tilde{\chi}_1(t) \exp[-(i/\hbar) \int \tilde{E}_1 dt] + a_2(t) \tilde{\chi}_2(t) \exp[-(i/\hbar) \int \tilde{E}_2 dt]$. The coefficients a_1 and a_2 satisfy

$$\begin{aligned} \dot{a}_1 &= M(t) \exp(i\theta(t)) a_2, \\ \dot{a}_2 &= -M(t) \exp(-i\theta(t)) a_1, \end{aligned} \quad (2)$$

where $\theta(t) = \int (\tilde{E}_1 - \tilde{E}_2) dt / \hbar$, $M(t) = m \delta / \{2[\delta^2 + m^2(t - t_a)^2]\}$ and $2\delta = \tilde{E}_2(t_a) - \tilde{E}_1(t_a)$. When the level splitting 2δ is small, the states are coupled only for a short time and if the phase change θ during this time is negligible, the solution of Eqs. (2) that satisfies $a_1(-\infty) = 1$, $a_2(-\infty) = 0$ is $a_1 = \cos(\int_{-\infty}^t M(t') dt')$, $a_2 = -\sin(\int_{-\infty}^t M(t') dt')$. Thus the probability of a transition from state 1 to state 2 is $|\sin(\int_{-\infty}^t M(t') dt')|^2 = 1$ and the probability of a transition from state 2 to state 1 is also 1. Because the character of the states changes at an anticrossing the effect of the transition is to preserve the character at the expense of the eigenstate number. In numerical data this appears as a rapid shift of weight from eigenstate n to $n \pm 1$. This result relies on $\theta(t)$ remaining small while the transition takes place and this is possible because the phase change during the time taken for the probability to reach $1 - \varepsilon$ is $\sim 2\delta^2/(\hbar m \varepsilon)$. The splitting 2δ is proportional to the barrier transmission coefficient⁵ so it is exponentially small when the barrier is high, therefore the phase change is small. The corrections to this approximate treatment are of order $\delta^2/(\hbar m) \sim \delta^2/(\hbar \omega U_0)$ and the exact Landau-Zener theory shows that the probability of the transition is actually $\exp(-2\pi\delta^2/(\hbar m)) \sim 1 - 2\pi\delta^2/(\hbar m)$.

The existence of anticrossings and a small number of bound states at $t \sim \tau/2$ is very important for accurate electron transfer. Ideally, Landau-Zener transitions would occur with probability one and there would be no other transitions. Then an initial state on one of the parabolic structures in Fig. 3 would follow the structure and undergo a change of localization at $t \sim \tau/2$, leading to transfer of one electron. In contrast, all the other states would undergo character preserving Landau-Zener transitions without a change of localization, leading to no electron transfer. When the Fermi level was swept through these states the net electron transfer would stay constant leading to plateaus of the form shown in Fig. 1.

The net electron transfer, summed up to the Fermi level, is insensitive to perturbations to the idealized sequence of transitions. This can be shown by expressing the time evolution operator $U(t_0 + \tau, t_0)$ in the instantaneous eigenstate basis and factorizing it in the form $U(t_0 + \tau, \tau/2 + t_0) U(\tau/2 + t_0, t_0)$. If the effects of propagating states and barrier penetration are negligible, the net electron transfer is $\sum_{i \in R} \sum_{j \in L, E_j \leq E_F} |U_{ij}(t_0 + \tau, t_0)|^2$, where R is the set of states bound on the right or of right character and L is defined

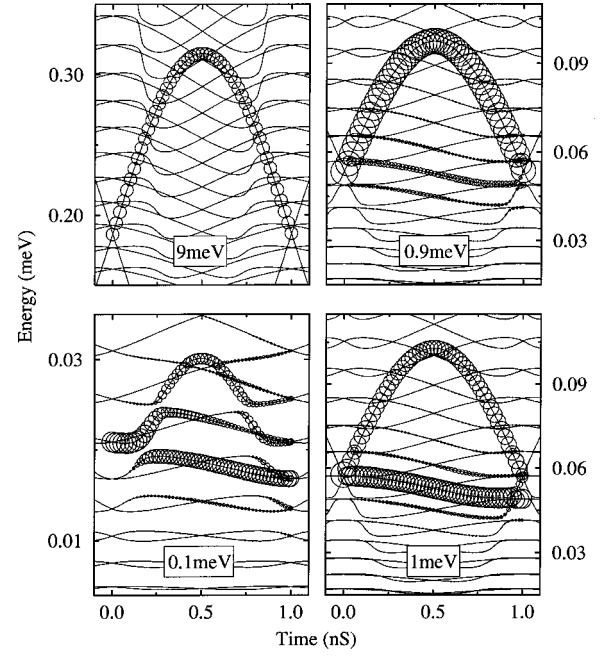


FIG. 4. Evolution of wave function ψ and time dependence of instantaneous eigenvalues. At each time, the circle areas represent the coefficients $|c_i|^2$ in the instantaneous eigenstate expansion of ψ .

similarly for the left side. Further, if the states in R and L couple appreciably only to bound states at $t = \tau/2 + t_0$, the electron transfer is

$$\begin{aligned} & \sum_{i \in R} \sum_{k \in L, E_k \leq E_F} \left| \sum_{j \in B} U_{ij}[t_0 + \tau, \tau/2 + t_0] U_{jk}(\tau/2 + t_0, t_0) \right|^2 \\ &= \sum_{j \in B} \sum_{k \in L, E_k \leq E_F} |U_{jk}(\tau/2 + t_0, t_0)|^2, \end{aligned}$$

where B is the set of states bound at $t = \tau/2 + t_0$ and the last step follows from unitarity. Unitarity then ensures that the electron transfer at the first plateau is close to one in two cases: either if (a) only one state below E_F couples to the states in B or if (b) only one state in B couples to the states below E_F . One or other of these cases applies when Landau-Zener transitions occur with high probability thus the electron transfer is accurately quantized.

The actual time evolution is illustrated in Fig. 4. Each frame shows the evolution of the state that makes the largest contribution to the first plateau at various barrier heights. The areas of the circles indicate the squared coefficients $|c_i(t)|^2$ in the expansion $\sum_i c_i(t) \chi_i(x, t)$ of the computed wave function. The evolution is nearly ideal in the high barrier regime ($V_0 = 9$ meV). Then only one initial state contributes significantly to the plateau and this state is localized in a weak potential minimum on the left of the barrier. Subsequently, the system tends to be in one instantaneous eigenstate—the one circle at each time corresponds to $|c_i|^2 > 0.9977$. The change of the eigenstate number with time indicates that the evolution follows the idealized sequence of Landau-Zener transitions. The squared U elements for direct LR coupling are of order 10^{-15} or less and the sum rule in form (a) ensures that the first plateau height differs from 1 by about 6 parts in 10^7 , although the dominant $|c_i|^2$ differs from

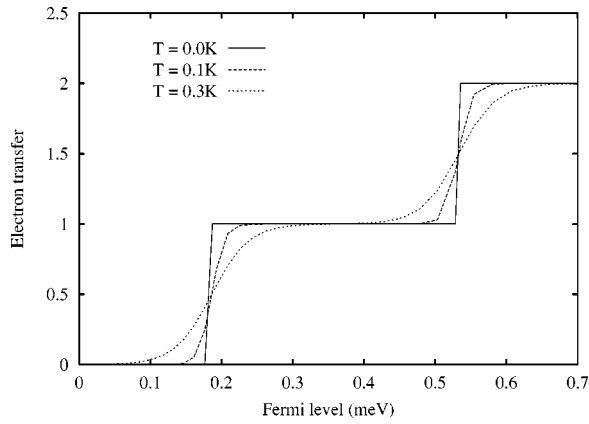


FIG. 5. Temperature dependence of the first two plateaus for the 9 meV barrier.

1 by about 2 parts in 1000. The evolution at lower barrier heights is less ideal ($V_0 = 0.9$ meV and 0.1 meV) and several terms are significant in the instantaneous eigenstate expansion. The evolution is also nonideal when two anticrossings are very close together at $t=0$ ($V_0 = 1$ meV). In these cases the sum rule in form (b) ensures that the first plateau height is still close to 1 unless V_0 is very small.

The accuracy of the quantization depends on barrier penetration in the initial states, the probability of Landau-Zener transitions, and the strength of direct LR coupling. All three effects are sensitive to the exponential tails of the right, left, and bound states and this is why the accuracy as a function of V_0 at fixed frequency is well fitted by $\alpha \exp(-\beta\sqrt{V_0})$. The high accuracy in the high barrier regime is partly due to the initial state having bound character and the binding is particularly strong when $V_0 = U_0$. In reality, the SAW amplitude sets an upper limit on U_0 but calculations for a wide range of model potentials are needed to determine whether an initial state of bound character is necessary for high accuracy. The important point is that the predicted accuracy is up to several orders of magnitude better than the required accuracy.

The effect of finite temperature is to reduce the accuracy but the reduction is small at typical experimental temperatures⁶ which are between 150 mK and 1.3 K. The states that correspond to the largest electron transfer have energies near the plateau edges, therefore the initial effect of increasing the temperature is to smooth the edges while keeping the electron transfer at the plateau center intact. This is illustrated in Fig. 5 for the 9 meV barrier whose accuracy is just below the minimum required for practical purposes. The effect of temperature is largest for systems with narrow

plateaus, for example the accuracy for the 9 meV barrier is 5.64×10^{-7} at 0 K and 6.18×10^{-6} at 150 mK. This is the worst case: higher barriers have broader plateaus and the effect of temperature is much less significant. In general, the electron transfer as a function of E_F for a large system at temperature, T , is

$$\int_0^\infty n(E)\rho(E)f(E, E_F, T)dE = - \int_0^\infty N(E) \frac{df(E, E_F, T)}{dE} dE,$$

where $n(E)$ is the transfer at energy E , $N(E)$ is the cumulative transfer, $\rho(E)$ is the density of states and f is the Fermi-Dirac function. When the temperature is low, $-df(E, E_F, T)/dE$ is sharply peaked at $E = E_F$, therefore the electron transfer at the plateau center remains close to the zero temperature value provided that the plateau width exceeds a few kT . This is the case in the high barrier regime.

The present results suggest it may be possible to use a time-dependent 1D channel as the basis of a quantum current standard, however, the effects of departures from 1D motion, disorder, electron-electron, and electron-phonon interactions remain to be investigated. It is not yet known whether these effects enhance or degrade accuracy but the accuracy predicted here exceeds the required accuracy by up to four orders of magnitude. So if a device that approached the conditions described here could be made, it could be usable even if departures from ideal conditions reduced its accuracy. Currently, the only type of device to which the theory might be relevant is the SAW device. Experiments with this type of device are done by sweeping a gate voltage to change the potential of the 1D channel relative to the Fermi level of the contacts. This results in quantized plateaus in the acoustoelectric current as a function of gate voltage. These plateaus could be similar to ones found theoretically when the Fermi level is swept. The theoretical plateaus occur because narrow bands of states are responsible for the majority of the electron transfer and the plateau edges correspond to the Fermi level passing through these bands. If similar bands of states exist in the experimental channel, plateaus would be seen when these bands pass through the Fermi level as the gate voltage is swept. The best accuracy in current SAW devices is 50 parts per million.⁷ The present results, which are not restricted to SAW devices, suggest it may be possible to engineer a device with better accuracy.

I thank Dr V. I. Talyanskii for explaining the SAW device and critically reading the manuscript. I am grateful for helpful discussions with him and Dr C. H. W. Barnes, Professor J. L. Beeby, J. Cunningham, Dr C. J. B. Ford, Professor M. Pepper, A. Robinson, and Dr J. Shilton. I thank Dr D. E. Khmelnitskii for drawing my attention to Ref. 4.

¹M. W. Keller, J. M. Martinis, and R. L. Kautz, *Phys. Rev. Lett.* **80**, 4530 (1998).

²V. I. Talyanskii, J. M. Shilton, M. Pepper, C. G. Smith, C. J. B. Ford, E. H. Linfield, D. A. Ritchie, and G. A. C. Jones, *Phys. Rev. B* **56**, 15 180 (1997).

³G. R. Aizin, G. Gumbs, and M. Pepper, *Phys. Rev. B* **58**, 10 589 (1998).

⁴C. Zener, *Proc. R. Soc. London, Ser. A* **137**, 696 (1932); L. Lan-

dau, *Phys. Z. Sowjetunion* **2**, 46 (1932).

⁵See, for example, L. D. Landau and E. M. Lifschitz, *Quantum Mechanics* (Pergamon, Oxford, 1977).

⁶V. I. Talyanskii, J. M. Shilton, J. Cunningham, M. Pepper, C. J. B. Ford, E. H. Linfield, D. A. Ritchie, and G. A. C. Jones, *Physica B* **251**, 140 (1998).

⁷V. I. Talyanskii (private communication).